

# Characterizing the Adsorption of Proteins on Glass Capillary Surfaces Using Electrospray-Differential Mobility Analysis

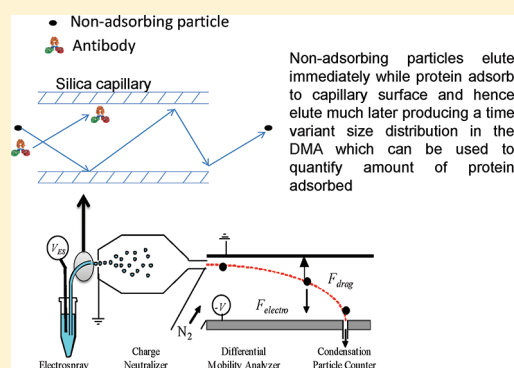
Suvajyoti Guha,<sup>†,‡</sup> Joshua R. Wayment,<sup>‡</sup> Mingdong Li,<sup>†,‡</sup> Michael J. Tarlov,<sup>‡</sup> and Michael R. Zachariah<sup>\*,†,‡</sup>

<sup>†</sup>Department of Mechanical Engineering and Department of Chemistry and Biochemistry, University of Maryland, College Park, Maryland 20742, United States

<sup>‡</sup>National Institute of Standards and Technology, Gaithersburg, Maryland 20899, United States

**S** Supporting Information

**ABSTRACT:** We quantify the adsorption and desorption of a monoclonal immunoglobulin-G antibody, rituximab (RmAb), on silica capillary surfaces using electrospray-differential mobility analysis (ES-DMA). We first develop a theory to calculate coverages and desorption rate constants from the ES-DMA data for proteins adsorbing on glass capillaries used to electrospray protein solutions. This model is then used to study the adsorption of RmAb on a bare silica capillary surface. A concentration-independent coverage of  $\approx 4.0 \text{ mg/m}^2$  is found for RmAb concentrations ranging from 0.01 to 0.1 mg/mL. A study of RmAb adsorption to bare silica as a function of pH shows maximum adsorption at its isoelectric point (pI of pH 8.5) consistent with literature. The desorption rate constants are determined to be  $\approx 10^{-5} \text{ s}^{-1}$ , consistent with previously reported values, thus suggesting that shear forces in the capillary may not have a considerable effect on desorption. We anticipate that this study will allow ES-DMA to be used as a “label-free” tool to study adsorption of oligomeric and multicomponent protein systems onto fused silica as well as other surface modifications.



## 1. INTRODUCTION

Protein adsorption is important to many fields, including biomaterials and bioprocessing, which has led to many studies to quantify it. The characterization methods employed can be broadly characterized into solution depletion, optical, spectroscopic, imaging and surface force measurement techniques.<sup>1,2</sup> Most of these techniques operate at stagnant conditions<sup>3,4</sup> or at low shear<sup>5,6</sup> (typically  $10^2$ – $10^3 \text{ s}^{-1}$ ) and have only rarely<sup>7–9</sup> been used for studying competitive adsorption of protein oligomers (i.e., monomers, dimers, trimers, etc., of the same protein).

An understanding of both the effects of shear and competitive adsorption is a relatively unexplored problem. It has been reported for example that shear flows increase protein adsorption,<sup>6</sup> which is obviously of interest in the context of the human circulatory system, where shear rates can vary from 1 to  $10^5 \text{ s}^{-1}$ .<sup>10</sup> However, while protein aggregation has been studied at high shear flow rates ( $10^6 \text{ s}^{-1}$ ),<sup>11,12</sup> adsorption to surfaces is yet to be probed under these conditions. Further, it is generally believed that in multicomponent systems, smaller proteins adsorb fastest, which are then displaced by larger ones.<sup>3–6</sup> This effect has been observed in both stagnant<sup>3,4</sup> and low shear flow conditions ( $\approx 500$ ,  $225$ – $2700 \text{ s}^{-1}$ ).<sup>5,6</sup> However, with a few exceptions,<sup>7–9</sup> there seems to be an overall lack of tools that can study adsorption—desorption of oligomers of the same protein. Furthermore, it is common to label proteins while studying multiprotein systems or sequential adsorption,<sup>13–16</sup> despite the fact that labeling may change

the conformational stability of proteins and also affect adsorption patterns.<sup>17–19</sup>

The objective of this paper is to demonstrate that electrospray-differential mobility analysis (ES-DMA), which has recently been used as a tool for characterizing nanoparticles, proteins, and viruses,<sup>20–24</sup> can also be used for studying protein adsorption. ES-DMA, also popularly known as gas-phase electrophoretic molecular mobility analysis (GEMMA),<sup>20</sup> comprises primarily three major components, an electrospray (ES) for aerosolizing particles into gas phase, a differential mobility analyzer (DMA) that operates at ambient conditions and characterizes particles based on a balance of drag and electrical force (i.e., it measures electrical mobility),<sup>25</sup> and a condensation particle counter (CPC). In prior work<sup>21,26</sup> we had observed size distributions of proteins to be time dependent, implying interaction of proteins with the ES capillary. It had also been demonstrated that the ES-DMA is capable of quantifying and resolving the oligomer distributions of proteins such as insulin and antibodies.<sup>21,26</sup> Thus ES-DMA offers the possibility to study competitive or sequential adsorption of oligomers of the same protein or a mixture of different proteins or both (as long as their sizes are different) without the need for labeling. Because of the ES, particles (proteins in this context) pass

**Received:** July 20, 2011

**Revised:** September 7, 2011

**Published:** September 09, 2011

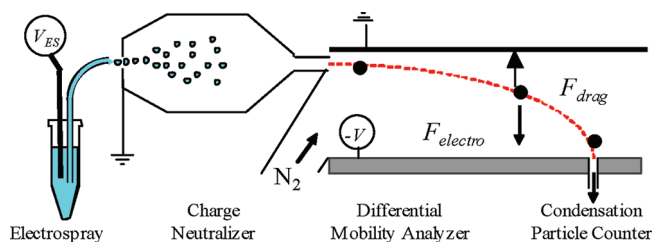


**Figure 1.** Schematic of the different components of the ES-DMA system. Solution is passed through a fused silica capillary under pressure and then electro sprayed into droplets containing protein. The protein-containing droplets pass through a Po-210 neutralizer, where solvent from droplets evaporates, droplets collide with positively and negatively charged gas species, and the protein analyte exits the neutralizer bearing either a single positive or negative or neutral charge. Particles are classified by differential mobility and counted by a condensation particle counter.

through a silica capillary under high shear (typically  $10^5 \text{ s}^{-1}$ ), thus offering the possibility of studying the effects of protein adsorption at high shear.

In this paper, we lay down the groundwork for using ES-DMA to study protein adsorption by studying the adsorption of rituximab (RmAb), a model monoclonal antibody,<sup>27</sup> to fused silica ES capillaries.

## 2. MATERIALS AND METHODS

**2.1. Protein Sample Preparation.** Buffer solutions for ES-DMA experiments were prepared by adding 0.77 g of ammonium acetate powder (Sigma Aldrich, St Louis, MO, #631-61-8) to 0.5 L of nanopure water (18 M $\Omega$ /cm, Barnstead nanopure UV system).<sup>28</sup> The pH was adjusted by addition of either glacial acetic acid (Mallinckrodt, Phillipsburg, NJ, #2504-14) or ammonium hydroxide (Baker, Phillipsburg, NJ, #9721-01).

The monoclonal antibody (IgG1) rituximab (RmAb) was purified using a protein A affinity column (GE Healthcare) and stored at  $-20^\circ\text{C}$  in 0.025 mol/L Tris buffer at pH 7.4, and  $1 \times 10^{-5}$  mol/L of  $\text{NaN}_3$  was added as a preservative. To desalt the protein sample, a Millipore centrifuge filter (30 kDa molecular weight cutoff) was used immediately prior to ES-DMA analysis at 13 200 rpm for 12 min. For ES-DMA experiments, RmAb was prepared at a concentration of 1.0 mg/mL, as determined by UV–vis absorption measurements in 0.020 mol/L ammonium acetate at pH 7, and further diluted to 0.01, 0.02, 0.05, and 0.1 mg/mL. For the “proof of principle” experiment described in section 3.1, a solution of 0.001% sucrose and 0.01 mg/mL RmAb was prepared with 0.020 mol/L ammonium acetate at pH 7.0.

**2.2. Capillary Surface Preparation.** For the electro spray source and adsorption studies, fused silica capillaries (inner diameter 25  $\mu\text{m}$ , outer diameter of 175  $\mu\text{m}$ , length 24 cm) were used. About 1.0 M  $\text{H}_2\text{SO}_4$  was flowed through the capillaries for 20–30 min (equivalent to 11–16 capillary volumes), followed by 18 M $\Omega$ /cm ultrapure water for another 10 min (5–6 capillary volumes). Prior to ES-DMA experiments, capillaries were cleaned by flowing 0.020 mol/L ammonium acetate buffer solutions at pH 7.0 for 5–10 min before introduction of the desired sample. Capillaries undergoing this treatment are referred to as “bare”. For all experiments, including the capillary cleanup step, the ES capillary pressure drop was maintained at 3.7 psi, which resulted in a capillary liquid flow rate of  $\approx 66 \text{ nL/min}$ .

**2.3. ES-DMA.** An electro spray (TSI, Inc., Shore View, MN, #3480) source was used to aerosolize the protein solutions. The electro sprayed droplets were charge reduced with a Po-210 radiation source so that most aerosol will have +1, 0, or  $-1$  charges.<sup>29</sup> This charge distribution

on particles are size-dependent and follow a Boltzmann distribution, and hence, the total particles in the gas phase can be quantified (this quantification will henceforth be referred to as “charge correction”) by collecting the singly charged particles. This charge correction was employed on all experiments other than the proof of principle experiment in section 3.1. A negative voltage was applied at the DMA (TSI, Inc., #3080) such that the +1 charged proteins would pass through the DMA and be counted by a condensation particle counter (CPC) (TSI, Inc., #3025A). A more detailed discussion about the technique is available elsewhere.<sup>21–24</sup> Figure 1 provides a schematic of the different components.

The ES-DMA was operated with a sheath flow rate of 10 L/min using nitrogen and an aerosol flow rate of  $\approx 1.5 \text{ L/min}$  using air. Size distributions of RmAb were obtained by scanning from 7.2 to 15.5 nm. The CPC was operated at a high flow mode of 1.5 L/min.

For the 25  $\mu\text{m}$  capillaries and the nominal flow rates used in this study, the shear rate is calculated to be  $\approx 10^4 \text{ s}^{-1}$ . This value is about 1 order of magnitude higher than techniques previously used to study protein adsorption under shear flow conditions such as total internal reflection fluorescence (TIRF),<sup>30</sup> ellipsometer,<sup>6</sup> and surface plasmon resonance.<sup>31</sup> The calculations for determination of shear rates are presented in the Supporting Information.

A typical adsorption–desorption experiment would constitute the following steps: first, insertion of the sample was followed by starting data collection after 4 min, to allow for the sample to elute through the capillary, pass through DMA, and get counted by the CPC; mobility distributions were obtained every 90 s (unless otherwise mentioned) until steady-state was achieved (within experimental variability); and finally, the protein sample was replaced with buffer, and further mobility distributions were obtained. The system was calibrated for size using 60 nm NIST calibrated polystyrene latex particles.<sup>32</sup>

It should be noted that all experiments described in section 3.2 onward did not incorporate sucrose as a marker, the gas phase data were charge corrected, and mobility distributions were obtained from 7.37 to 15.1 nm using commercial TSI Inc. software (Aerosol Instrument Manager) that allowed us to obtain size distributions more frequently (every 90 s) compared to the experiment in section 3.1. Also, because the ES community (especially mass spectrometry) uses different capillary diameters and hence the flow volume can vary significantly,<sup>33–35</sup> we will replace time with equivalent capillary volume, which is defined by the product of time and capillary flow rate divided by the total volume within the capillary. In this regard, the mass-spectrometry community typically uses different passivations on silica surfaces to reduce protein adsorption, which concomitantly reduces the wait times for protein breakthrough.<sup>36</sup>

## 3. RESULTS AND DISCUSSION

**3.1. Proof of Principle.** In our prior work using ES-DMA for characterization of proteins,<sup>21,26</sup> evidence for adsorption of proteins to the bare capillary surfaces was manifested by changes in the measured mobility distributions as a function of elution time from the capillary. In this paper we systematically explore these effects and demonstrate how ES-DMA can be used to study interactions between proteins and the glass capillary surface. Sucrose was used as a reference marker (in this regard, sucrose has also previously been used with protein to investigate the mechanism of ES droplet formation<sup>37</sup>) in this experiment because it does not significantly interact with the silica surface of the capillary at pH 7. On the other hand, any protein that interacts with the capillary will result in a mobility distribution that should vary with time.

Figure 2A plots the size distributions from 3 to 13 nm obtained at times of 0, 99, 128, 137.5, and 175.5 min for a mixture of

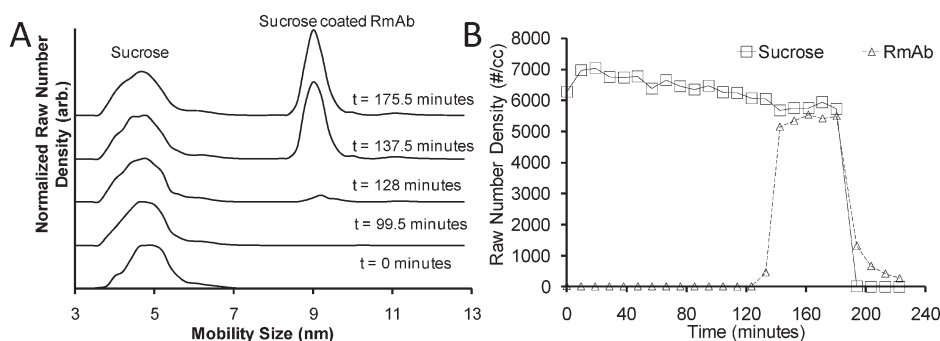


**Figure 2.** (A) Size distributions of 0.001% sucrose (v/v) mixed with 0.01 mg/mL RmAb at pH 7.0 using the ES-DMA as a function of time. Other time points have not been shown for clarity. The data has been normalized with respect to the sucrose peak. (B) The integration of the sucrose peak (open square, line) and RmAb peak (open triangle, dotted line) plotted as a function of time. It includes the adsorption phase (up to  $\approx 140$  min), the steady state phase (up to  $\approx 180$  min), and the desorption phase (up to  $\approx 230$  min).

0.001% sucrose (v/v) and 0.01 mg/mL RmAb. At  $t = 0$  and 99 min, a peak for sucrose at 4.6 nm is clearly observed, while no peak is observed for RmAb. At  $t = 128$  min, a peak for RmAb at  $\approx 9$  nm is first observed that increases quickly in intensity to a steady-state value with time. These results show that sucrose does not bind to the capillary, and protein adsorption occurs over a long period of time. The RmAb mobility size after correcting for sucrose that coats the RmAb molecule<sup>38</sup> is in agreement with previously reported values<sup>20,21</sup> for immunoglobulin. Figure 2A also shows small quantities of RmAb dimers at 11.2 nm, which appears because of an electrospray artifact of two monomers in the same ES droplet.<sup>39</sup>

After the protein signal has reached steady state ( $\approx 180$  min), the protein solution is replaced with a 20 mmol/L ammonium acetate buffer at pH 7. Upon replacing the sample with buffer, the sucrose signal decreases immediately; in contrast, the RmAb signal decays relatively slowly. This is evident from Figure 2B, which plots the integrated area under the RmAb and sucrose peak as a function of time for the entire experiment.

These results are summarized and interpreted as follows. The presence of sucrose signal together with the absence of RmAb signal suggests that RmAb adsorbs to the wall of the glass capillary. From 0 to  $\approx 130$  min RmAb adsorbs until the RmAb surface coverage reaches saturation, at which point protein is first observed and the signal rapidly reaches steady-state. Upon replacing the protein/sucrose solution with pure ammonium acetate buffer, the sucrose signal decreases rapidly, while the RmAb signal falls more slowly. The slowly decaying RmAb signal suggests slow desorption of RmAb from the glass capillary surface.

**3.2. Surface Coverage and Adsorption Kinetics.** We will now set forth the relationships necessary to extract kinetic parameters and surface coverages from the mobility distributions. The reader is reminded that RmAb does not elute from the ES capillary for many minutes (or capillary volumes) for all experiments conducted for this work; hence, we are not in a position to determine the adsorption rate constants for RmAb.

To determine the surface coverage, we define  $C_{\text{eluting}}^{t(i)}$  as the concentration of protein in liquid phase eluting through the ES capillary, a parameter that varies with time, where superscript  $t(i)$  denotes time  $i$ . The DMA-CPC however measures the gas-phase concentration, which must be corrected for transport losses and particle charging fraction.<sup>21</sup> While the charge fraction is based on well-known relationships<sup>21,24,40</sup> that allow one to make the appropriate quantitative corrections (defined by  $\alpha_{\text{charge}}$ ), the transport losses must be empirically calibrated, through a parameter  $\alpha$ , which

takes into account Brownian motion<sup>41</sup> and electrostatic deposition losses and electrospray efficiency<sup>42</sup> as shown in eq 1

$$C_{\text{eluting}}^{t(i)} = \alpha C_{\text{gas phase}}^{t(i)} \frac{Q_{\text{cpc}}}{Q_{\text{capillary}}} \quad (1)$$

where  $\alpha$  is an unknown at this point since  $C_{\text{eluting}}^{t(i)}$  is unknown, and  $Q_{\text{cpc}}$  and  $Q_{\text{capillary}}$  are the flow rates inside the CPC and capillary respectively.  $C_{\text{gas phase}}^{t(i)}$  is given by eq 2 and is determined by charge correcting the CPC raw data and then integrating over the entire size range of observed protein species, such as protein monomer, dimer, or larger aggregates.

$$C_{\text{gas phase}}^{t(i)} = \int \frac{d(\alpha_{\text{charge}} N_{\text{cpc}}^{t(i)})}{dD_p} dD_p \quad (2)$$

where  $N_{\text{cpc}}^{t(i)}$  are the counts obtained by the CPC at a mobility diameter of  $D_p$ ,  $dD_p$  is the increment in mobility diameter, and  $\alpha_{\text{charge}}$  accounts for the charge correction.<sup>21,24,40</sup> For RmAb the monomer and dimer counts are obtained by integrating from 7.6 to 9.6 nm and 9.8 to 11.8 nm, respectively.

When the concentration of eluting protein reaches steady state (or in other words assuming *adsorption reaches equilibrium*)  $C_{\text{eluting}}^{t(\text{ss})}$  can be written as shown below

$$C_{\text{eluting}}^{t(\text{ss})} = C_{\text{solution}} \quad (3)$$

where  $C_{\text{solution}}$  is the total concentration of the protein in solution measured by an independent technique such as UV-vis and the superscript  $t(\text{ss})$  denotes steady state. Then, by combining eq 1 and 3,  $\alpha$  can be determined at steady state. Using this approach we find  $\alpha$  is  $\approx 4-5$  for RmAb at all concentrations and pH values; however, we have found that  $\alpha$  is dependent on system operating parameters, such as the aerosol flow and sheath flow as well as protein type (unpublished results). The assumption of equilibrium will be addressed in greater detail elsewhere (manuscript under preparation). To summarize the results from that work, we found that at steady-state conditions, the type of surface passivation only affected the time to reach steady state and had no effect on the measured size distributions. In addition, with serial dilution there was no change in the time dependence of RmAb elution from gelatin passivated surface, which implied little or no adsorption.

Recognizing that steady state corresponds to equilibrium allows us to evaluate the adsorption kinetics under nonequilibrium conditions, because  $\alpha$  once evaluated at steady state can

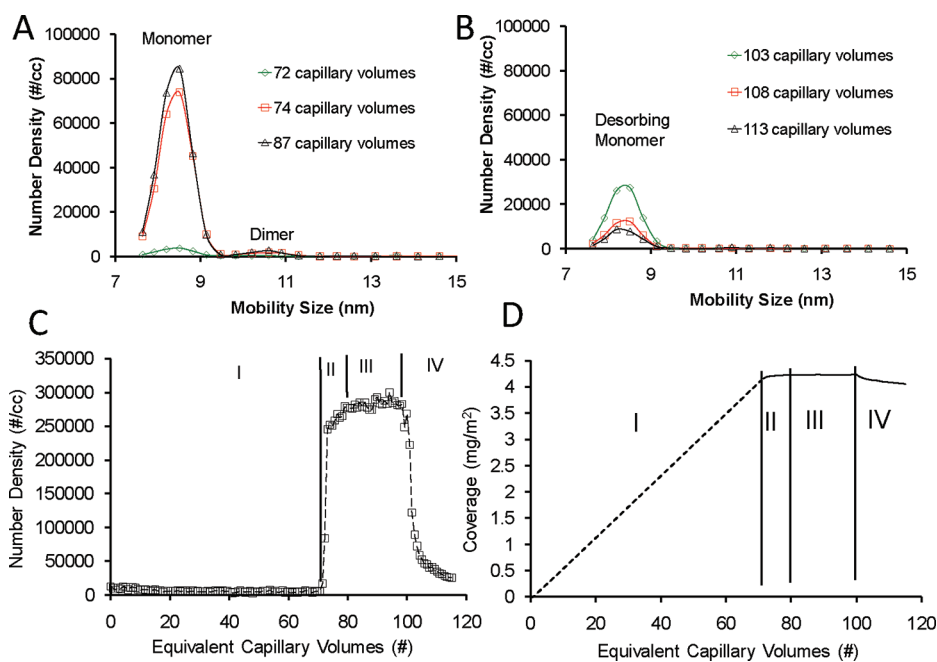


**Figure 3.** (A) Size distributions of RmAb in 20 mmol/L ammonium acetate at pH 7.0 as a function of time. (B) The size distribution as a function of time when the protein is replaced with buffer at the same ionic strength and pH. (C) Sum of the monomer and twice the dimer counts as a function of time (open square). (D) Surface coverage as a function of time for 0.01 mg/mL RmAb. The dotted line in domain I represents no protein eluting and thus the initial rate of protein adsorption is unknown. Refer to the text for a detailed discussion on domains I–IV.

then be used at other conditions, assuming linearity. Concomitantly, this also allows the amount of protein adsorbed to the capillary surface per unit area  $\Gamma_{\text{ads}}$  to be calculated. Because the amount of protein adsorbed varies with time and DMA scans require a finite dwell time ( $\Delta t$ ),  $\Gamma_{\text{ads}}^{t(i)}$  is evaluated over a given time interval and summed over each scan period as given by eq 4

$$\Gamma_{\text{ads}} = \sum \Gamma_{\text{ads}}^{t(i)} = \sum \frac{(C_{\text{solution}} - C_{\text{eluting}}^{t(i)}) Q_{\text{capillary}} \Delta t}{\pi D_{\text{capillary}} L_{\text{capillary}}} \quad (4)$$

where  $D_{\text{capillary}}$  and  $L_{\text{capillary}}$  are the diameter and length of the capillary, and  $\Gamma_{\text{ads}}$  is the total coverage obtained.<sup>43</sup>

When the protein is replaced with buffer,  $\Gamma_{\text{des}}^{t(i)}$  is the amount of protein desorbed at time period  $t(i)$  and is given by

$$\Gamma_{\text{des}} = \sum \Gamma_{\text{des}}^{t(i)} = \sum \frac{C_{\text{eluting}}^{t(i)} Q_{\text{capillary}} \Delta t}{\pi D_{\text{capillary}} L_{\text{capillary}}} \quad (5)$$

where  $\Gamma_{\text{des}}$  is the total amount of desorbed protein.

Figure 3A presents data for 0.01 mg/mL RmAb at pH 7 electrospayed through a bare capillary for up to  $\approx 100$  capillary volumes, while Figure 3B shows size distributions for RmAb as a function of time when the sample is replaced with buffer. In this case, RmAb first appears at  $\approx 72$  capillary volumes, consistent with results obtained before when sucrose was used as a “marker”. Figure 3C displays the total counts of RmAb as a function of time, and the plot is divided into four domains. Domain I is characterized by zero signal intensity due to the adsorption of nearly all protein to the glass capillary surface. Domain II is characterized by a rapid rise in counts following saturation of the RmAb surface coverage. Domain III is where RmAb signal reaches steady state. Domain IV is during buffer rinse, where a rapid decay in RmAb signal occurs. It should also be noted that the mobility size of the RmAb monomers and dimers obtained during desorption (domain IV) are equivalent to that obtained during adsorption

and that the desorbing species are primarily monomers, although from this measurement we cannot be certain that the desorbed monomer is in its native state. Figure 3D shows the resulting surface coverage ( $\text{mg}/\text{m}^2$ ) as a function of time, determined from eq 5. A maximum steady-state coverage of  $\approx 4 \text{ mg}/\text{m}^2$  is determined, which only slightly decreases during the desorption period. The next section compares the coverages with previously reported values.

**3.3. Concentration- and pH-Dependent Adsorption–Desorption of RmAb.** Having established the methodology to determine coverage and adsorption–desorption kinetics, we are now in a position to determine these parameters for different conditions. Experiments like those shown in Figure 3 were carried out at four different concentrations of RmAb: 0.01, 0.02, 0.05, and 0.1 mg/mL at pH 7.0. The capillary volume at which RmAb started eluting was found to be inversely proportional to solution concentration, as shown in Figure 4A. For example, at 0.01 mg/mL the first evidence of RmAb appears at  $\approx 72$  capillary volumes, as shown in Figure 3C before; likewise, RmAb starts eluting after  $\approx 38$  capillary volumes,  $\approx 13$  capillary volumes, and  $\approx 7$  capillary volumes for 0.02, 0.05, and 0.1 mg/mL, respectively. It is also evident from Figure 4A that the total gas phase counts linearly correlates with the liquid phase concentration; i.e., the gas phase density of 0.02, 0.05, and 0.1 mg/mL solutions after steady state are about 2, 5, and 10 times that of the steady-state gas-phase density of 0.01 mg/mL (shown in Figure 3C) solution, implying that the recovery in all these cases is the same and that the ES-DMA is linear in this concentration range. Size distributions were obtained for 15–20 capillary volumes after steady state had been attained for each of the above cases, after which the RmAb samples were replaced with buffer and size distributions obtained for  $\approx 15$  capillary volumes, to determine the desorption rate. The same methodology was adopted for the pH study.

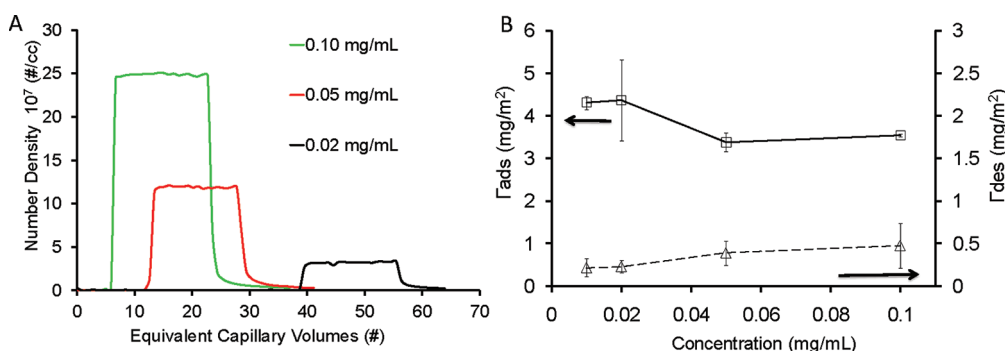


**Figure 4.** (A) The total gas-phase density of RmAb as a function of time expressed in equivalent capillary volumes at four different concentrations at pH 7.0. For clarity only one set of experiments has been shown. Refer to Figure 3C for 0.01 mg/mL concentration. (B) Adsorbed (open square) and desorbed amounts (open triangle, dotted line) of RmAb per unit area as a function of concentration.

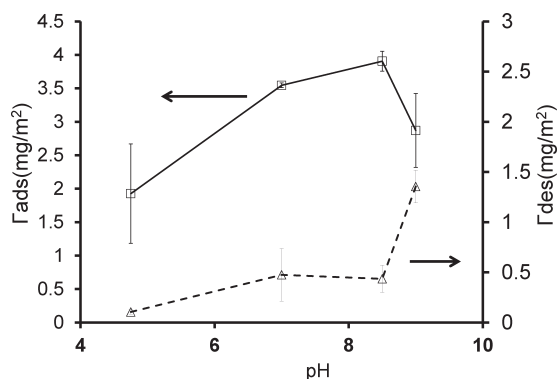


**Figure 5.** Adsorbed (open square) and desorbed RmAb (open triangle, dotted line) per unit area as a function of pH at a concentration of 0.1 mg/mL.

Using eqs 4 and 5, the surface coverage of RmAb on the glass capillary surface and the amount desorbed are plotted as a function of RmAb solution concentration in Figure 4B. The error bars are standard deviations determined from two or three experiments. Within experimental uncertainty, the amounts of both adsorbed and desorbed RmAb appear to be relatively independent of protein concentration.

In contrast to our finding that protein adsorption remains approximately constant as a function of concentration, other groups have reported that protein adsorption increases as a function of concentration under both stagnant and high shear flow conditions.<sup>44–48</sup> Nonetheless, the coverages of 3.5–4.3 mg/m<sup>2</sup> determined here for concentrations ranging from 0.01 to 0.1 mg/mL fall within the range of 2–18 mg/m<sup>2</sup> reported in the literature for silica surfaces.<sup>44–53</sup> The reasons for the breadth of values may be attributed to differences in surface properties,<sup>54</sup> ionic strength,<sup>44,55,56</sup> pH,<sup>51,52,55,57</sup> and different immunoglobulins.<sup>51</sup>

Using simple structural models for RmAb, we can estimate if adsorption is monolayered or multilayered. For a typical IgG, the projected side (53 nm<sup>2</sup>) and frontal areas (94 nm<sup>2</sup>)<sup>21</sup> give corresponding coverages of 4.6 and 2.6 mg/m<sup>2</sup>, respectively. Our experimental values of 3.5–4.3 mg/m<sup>2</sup> fall within this range, suggesting approximately monolayer coverage for RmAb on the glass capillary surface; however, we cannot exclude the possibilities of mixed orientations or coverages, or surface-induced aggregation or conformation changes that would change the adsorbed area of the protein.<sup>44,57–60</sup> Many studies have proposed monolayer adsorption,

even for coverages up to 18 mg/m<sup>2</sup> for IgG,<sup>57,61,62</sup> although multilayer adsorption has been reported by many others.<sup>55,59,63–66</sup>

The effect of pH on adsorption of RmAb was also examined. Figure 5 shows the amount of RmAb adsorbed (primary axis) and desorbed per unit area (secondary axis) of the capillary as a function of pH at a concentration of 0.1 mg/mL, and error bars were obtained by obtaining data at least in duplicate. We observe the highest surface coverage near the isoelectric point (pI) of the protein. These results are consistent with the dome-shaped profile commonly reported by others,<sup>51,56,64</sup> suggesting that intermolecular electrostatic repulsion effects may be important in influencing protein surface coverage. It should be pointed out that the pH study was limited to pH 9.0 since at  $\approx$ pH 10.0 we observed etching of the silica capillaries that produced significant noise in the size distribution.

We also quantify the desorbed RmAb at pH 4.75, 7.0, 8.5, and 9.0 to be  $0.11 \pm 0.02$ ,  $0.48 \pm 0.26$ ,  $0.44 \pm 0.13$ , and  $1.35 \pm 0.16$  mg/m<sup>2</sup>, respectively, which translates to 5.5%, 15.3%, 11.1%, and 47% of the amounts adsorbed. Buijs et al.<sup>51</sup> using reflectometry found  $\approx$ 10% desorption of IgG from silica, consistent with our findings.

**3.4. Desorption Rate Constants.** On the basis of the desorption data, we can also extract kinetic rate constants. Assuming that desorption over the 90 s scan time is constant, we can determine the number of particles that desorb,  $N_{\text{desorb,gas}}^{t(i)}$ , by integrating the area under the monomer peak. Then the number of particles desorbing is  $N_{\text{desorb,liquid}}^{t(i)}$ , such that

$$N_{\text{desorb,liquid}}^{t(i)} = N_{\text{desorb,gas}}^{t(i)} Q_{\text{cpc}} \Delta t_i \alpha \quad (6)$$

At any time  $t(i)$ , the amount of particles remaining on the surface, denoted by  $N_{\text{surface}}^{t(i)}$ , is

$$N_{\text{surface}}^{t(i)} = N_{\text{surface}}^{\text{total}} - N_{\text{desorb,liquid}}^{t(i)} \quad (7)$$

where the total number of particles on the surface,  $N_{\text{surface}}^{\text{total}}$ , is calculated from the size distribution as determined by the DMA, the area of the capillary, and assuming monolayer coverage.

The desorption rate is the change of surface concentration with time, which we assume to be a first-order process, and is integrated to give

$$\log \left( \frac{N_{\text{surface}}^{t(i)}}{N_{\text{surface}}^{\text{total}}} \right) = -K_{\text{desorption}} (t(i) - 0) \quad (8)$$

where  $K_{\text{desorption}}$  is the desorption rate constant.

Using eq 8, the rate constants of desorption for the concentrations studied were found to be  $\approx 10^{-5}$  s<sup>-1</sup> and invariant of

**Table 1. Desorption Rate Constants at Different Concentrations and pH Values**

concentration (mg/mL) varied at pH 7.0	desorption rate constants ( $s^{-1}$ )	pH varied at concentration 0.1 mg/mL	desorption rate constants ( $s^{-1}$ )
0.01	$1.8 \times 10^{-5} \pm 7.1 \times 10^{-6}$	4.5	$2.2 \times 10^{-5} \pm 2.5 \times 10^{-6}$
0.02	$1.9 \times 10^{-5} \pm 1.0 \times 10^{-5}$	7.0	$2.7 \times 10^{-5} \pm 4.2 \times 10^{-6}$
0.05	$1.9 \times 10^{-5} \pm 3.5 \times 10^{-6}$	8.5	$2.7 \times 10^{-5} \pm 1.4 \times 10^{-6}$
0.1	$1.7 \times 10^{-5} \pm 2.4 \times 10^{-6}$	9.0	$1.2 \times 10^{-4} \pm 5.8 \times 10^{-6}$

concentration. The desorption rate constants at pH 4.75, 7.0, and 8.5 were determined to be  $\approx 10^{-5} s^{-1}$ , whereas for pH 9 it was  $\approx 10^{-4} s^{-1}$ . The higher desorption rate at pH 9.0 may be caused by electrostatic repulsion between the silica and adsorbed protein. The desorption rate constants are listed in Table 1. Using X-ray photoelectron spectroscopy, Ball et al.<sup>58</sup> found the desorption rate constant for IgG to be  $\approx 10^{-5} s^{-1}$ , consistent with our results. Because the experiments by Ball et al. were performed under stagnant conditions, the reasonable agreement of results implies that shear does not considerably affect the desorption rate constant for RmAb on a glass capillary surface.

#### 4. CONCLUSIONS

The ES-DMA method offers the possibility to study “label-free” competitive as well as sequential adsorption of oligomers of the same proteins and or multiple proteins under high shear ( $\approx 10^4 s^{-1}$ ). We perform pH (4.75–9.0) and concentration-based studies for RmAb (0.01–0.1 mg/mL), a monoclonal antibody. Concentration does not seem to have an effect on the amount of protein adsorbed at high shear flow conditions. The pH studies show maximum adsorption around the *pI* of the protein, consistent with the literature. The desorption rate constants were found to be consistent with other studies at static conditions, implying that shear may not have a significant effect on desorption kinetics. It should be mentioned that this methodology can also, in principle, be adapted by the mass spectrometry community for studying protein adsorption–desorption on and from silica capillaries, although because the number of charges on proteins would be solution pH specific, quantitation of adsorption–desorption would be more complicated. Such an issue does not arise for the ES-DMA, since a Po-210 charge neutralizer is used. In a future work, we will extend the applications of ES-DMA by quantifying competitive adsorption–desorption of IgM monomers and dimers onto fused silica and modified silica surfaces.

#### ■ ASSOCIATED CONTENT

**Supporting Information.** Derivation of the shear rates inside a 25  $\mu m$  ES capillary at a capillary flow rate of 66 nL/min. This information is available free of charge via the Internet at <http://pubs.acs.org>.

#### ■ AUTHOR INFORMATION

##### Corresponding Author

\*Phone: 301.405.4311. Fax: 301.314.9477. E-mail: [mrz@umd.edu](mailto:mrz@umd.edu).

#### ■ REFERENCES

(1) Hlady, V.; Buijs, J.; Jennissen, H. P. *Methods Enzymol.* **1999**, *309*, 402–429.

- (2) Claesson, P. M.; Blomberg, E.; Froberg, J. C.; Nylander, T.; Arnebrant, T. *Adv. Colloid Interface Sci.* **1995**, *57*, 161–227.
- (3) Nylander, T.; Kekicheff, P.; Ninham, B. W. *J. Colloid Interface Sci.* **1994**, *164* (1), 136–150.
- (4) Elgersma, A. V.; Zsom, R. L. J.; Lyklema, J.; Norde, W. *J. Colloid Interface Sci.* **1992**, *152* (2), 410–428.
- (5) Wojciechowski, P.; Tenhove, P.; Brash, J. L. *J. Colloid Interface Sci.* **1986**, *111* (2), 455–465.
- (6) Ortega-Vinuesa, J. L.; Tengvall, P.; Walivaara, B.; Lundstrom, I. *Biomaterials* **1998**, *19* (1–3), 251–262.
- (7) Lensen, H. G. W.; Bargeman, D.; Bergveld, P.; Smolders, C. A.; Feijen, J. *J. Colloid Interface Sci.* **1984**, *99* (1), 1–8.
- (8) Okubo, M.; Azume, I.; Yamamoto, Y. *Colloid Polym. Sci.* **1990**, *268* (7), 598–603.
- (9) Zsom, R. L. J. *J. Colloid Interface Sci.* **1986**, *111* (2), 434–445.
- (10) Trusky, G. A.; Yuan, F.; Katz, D. F., *Transport Phenomena in Biological System*; Pearson Education: Upper Saddle River, NJ, 2004.
- (11) Maa, Y. F.; Hsu, C. C. *Biotechnol. Bioeng.* **1997**, *54* (6), 503–512.
- (12) Oliva, A.; Santovena, A.; Farina, J.; Llabres, M. *J. Pharm. Biomed. Anal.* **2003**, *33* (2), 145–155.
- (13) Holmberg, M.; Hou, X. L. *Langmuir* **2009**, *25* (4), 2081–2089.
- (14) Pitt, W. G.; Park, K.; Cooper, S. L. *J. Colloid Interface Sci.* **1986**, *111* (2), 343–362.
- (15) Borovetz, H. S.; Molek, G. E.; Levine, G.; Hardesty, R. L. *Biomed. Med. Adv. Artif. Organs* **1982**, *10* (3), 187–203.
- (16) Lecompte, M. F.; Rubinstein, I.; Miller, I. R. *J. Colloid Interface Sci.* **1983**, *91* (1), 12–19.
- (17) Elhorst, J. K.; Olthuis, F. M.; Bargeman, D.; Smolders, C. A.; Feijen, J. *Int J Artif Organs* **1978**, *1* (6), 288–292.
- (18) Grant, W. H.; Smith, L. E.; Stromberg, R. R. *J. Biomed. Mater. Res.* **1977**, *11* (1), 33–38.
- (19) Vanderscheer, A. T.; Feijen, J.; Elhorst, J. K.; Krugersdagheaux, P. G. L. C.; Smolders, C. A. *J. Colloid Interface Sci.* **1978**, *66* (1), 136–145.
- (20) Bacher, G.; Szymanski, W. W.; Kaufman, S. L.; Zollner, P.; Blaas, D.; Allmaier, G. *J. Mass Spectrom.* **2001**, *36* (9), 1038–1052.
- (21) Pease, L. F.; Elliott, J. T.; Tsai, D. H.; Zachariah, M. R.; Tarlov, M. J. *Biotechnol. Bioeng.* **2008**, *101* (6), 1214–1222.
- (22) Pease, L. F.; Lipin, D. I.; Tsai, D. H.; Zachariah, M. R.; Lua, L. H. L.; Tarlov, M. J.; Middelberg, A. P. *J. Biotechnol. Bioeng.* **2009**, *102* (3), 845–855.
- (23) Tsai, D. H.; Zangmeister, R. A.; Pease, L. F.; Tarlov, M. J.; Zachariah, M. R. *Langmuir* **2008**, *24* (16), 8483–8490.
- (24) Tsai, D. H.; Pease, L. F.; Zangmeister, R. A.; Tarlov, M. J.; Zachariah, M. R. *Langmuir* **2009**, *25* (1), 140–146.
- (25) Knutson, E. O.; Whitby, K. T. *J. Aerosol Sci.* **1975**, *6* (6), 443–451.
- (26) Pease, L. F.; Sorci, M.; Guha, S.; Tsai, D. H.; Zachariah, M. R.; Tarlov, M. J.; Belfort, G. *Biophys. J.* **2010**, *99* (12), 3979–3985.
- (27) <http://www.gene.com/gene/products/information/pdf/rituxan-prescribing.pdf>
- (28) Reference to commercial equipment, supplies, or software neither implies its endorsement by the National Institute of Standards and Technology (NIST) nor implies it to be necessarily best suited for this purpose. Views expressed in this article reflect those of the authors and do not constitute official positions of the U.S. Government.
- (29) Kim, S. H.; Woo, K. S.; Liu, B. Y. H.; Zachariah, M. R. *J. Colloid Interface Sci.* **2005**, *282* (1), 46–57.
- (30) Daly, S. M.; Przybycien, T. M.; Tilton, R. D. *Langmuir* **2005**, *21* (4), 1328–1337.
- (31) Green, R. J.; Davies, M. C.; Roberts, C. J.; Tendler, S. J. B. *Biomaterials* **1999**, *20* (4), 385–391.
- (32) Lall, A. A.; Ma, X. F.; Guha, S.; Mulholland, G. W.; Zachariah, M. R. *Aerosol Sci. Technol.* **2009**, *43* (11), 1075–1083.
- (33) Wytttenbach, T.; Kemper, P. R.; Bowers, M. T. *Int. J. Mass Spectrom.* **2001**, *212* (1–3), 13–23.
- (34) Chen, D. R.; Pui, D. Y. H.; Kaufman, S. L. *J. Aerosol Sci.* **1995**, *26* (6), 963–977.
- (35) Muller, R.; Laschober, C.; Szymanski, W. W.; Allmaier, G. *Macromolecules* **2007**, *40* (15), 5599–5605.

- (36) Razunguzwa, T. T.; Warriar, M.; Timperman, A. T. *Anal. Chem.* **2006**, *78* (13), 4326–4333.
- (37) Kaufman, S. L. *Anal. Chim. Acta* **2000**, *406* (1), 3–10.
- (38) Once the protein starts eluting, an ES droplet is constituted of both the protein as well as sucrose, and as the droplet starts drying up, the protein gets encrusted by the sucrose. The correct protein size can then be determined by using the following equation<sup>23</sup>  $d_{\text{RmAb}} = (d_{\text{RmAb,sucrose}}^3 - d_{\text{sucrose}}^3)^{1/3}$ , where  $d_{\text{RmAb,sucrose}}$  is the diameter of the RmAb coated with sucrose,  $d_{\text{sucrose}}$  is the diameter of the sucrose, and  $d_{\text{RmAb}}$  is the diameter of the protein after correcting for the sucrose encrusting the protein.
- (39) Li, M. D.; Guha, S.; Zangmeister, R. A.; Tarlov, M. J.; Zachariah, M. R. *Aerosol Sci. Technol.* **2011**, *45* (7), 849–860.
- (40) Wiedensohler, A. *J. Aerosol Sci.* **1988**, *19* (3), 387–389.
- (41) Friedlander, S. K. *Smoke, Dust and Haze: Fundamentals of Aerosol Dynamics*, 2nd ed.; Oxford University Press: New York, 2000.
- (42) Magnuson, M. L.; Urbansky, E. T.; Kelty, C. A. *Talanta* **2000**, *52* (2), 285–291.
- (43) Because after breakthrough of protein, RmAb attains steady state almost immediately, the adsorbed amount of protein can be more easily determined for the specific case of RmAb by using  $(C_{\text{solution}} Q_{\text{capillary}} \Delta t_{\text{breakthrough}}) / (\pi D_{\text{capillary}} L_{\text{capillary}})$ , where  $\Delta t_{\text{breakthrough}}$  is the time for the RmAb signal to breakthrough expressed in minutes. This however would then not be generic, since not all proteins show a similar breakthrough pattern, as we will show in a future work.
- (44) Jonsson, U.; Malmqvist, M.; Ronnberg, I. *Biochem. J.* **1985**, *227* (2), 373–378.
- (45) Silva, C. S. O.; Baptista, R. P.; Santos, A. M.; Martinho, J. M. G.; Cabral, J. M. S.; Taipa, M. A. *Biotechnol. Lett.* **2006**, *28* (24), 2019–2025.
- (46) Chuang, H. Y. K.; King, W. F.; Mason, R. G. *J. Lab. Clin. Med.* **1978**, *92* (3), 483–496.
- (47) Fair, B. D.; Jamieson, A. M. *J. Colloid Interface Sci.* **1980**, *77* (2), 525–534.
- (48) Brash, J. L.; Lyman, D. J. *J. Biomed. Mater. Res.* **1969**, *3* (1), 175–189.
- (49) Bee, J. S.; Chiu, D.; Sawicki, S.; Stevenson, J. L.; Chatterjee, K.; Freund, E.; Carpenter, J. F.; Randolph, T. W. *J. Pharm. Sci.* **2009**, *98* (9), 3218–3238.
- (50) Bremer, M. G. E. G.; Duval, J.; Norde, W.; Lyklema, J. *Colloids Surf., A* **2004**, *250* (1–3), 29–42.
- (51) Buijs, J.; vandenBerg, P. A. W.; Lichtenbelt, J. W. T.; Norde, W.; Lyklema, J. *J. Colloid Interface Sci.* **1996**, *178* (2), 594–605.
- (52) Buijs, J.; White, D. D.; Norde, W. *Colloids Surf., B* **1997**, *8* (4–5), 239–249.
- (53) Kamyshny, A.; Toledano, O.; Magdassi, S. *Colloids Surf., B* **1999**, *13* (4), 187–194.
- (54) Iler, R. K. *The Chemistry of Silica*; Wiley Interscience: New York, 1979; Chapter 6, pp 626–627.
- (55) Hook, F.; Rodahl, M.; Kasemo, B.; Brzezinski, P. *Proc. Natl. Acad. Sci. U. S. A.* **1998**, *95* (21), 12271–12276.
- (56) Ramsden, J. J.; Prenosil, J. E. *J. Phys. Chem.* **1994**, *98* (20), 5376–5381.
- (57) Bagchi, P.; Birnbaum, S. M. *J. Colloid Interface Sci.* **1981**, *83* (2), 460–478.
- (58) Ball, V.; Bentaleb, A.; Hemmerle, J.; Voegel, J. C.; Schaaf, P. *Langmuir* **1996**, *12* (6), 1614–1621.
- (59) Jung, L. S.; Campbell, C. T.; Chinowsky, T. M.; Mar, M. N.; Yee, S. S. *Langmuir* **1998**, *14* (19), 5636–5648.
- (60) Beissinger, R. L.; Leonard, E. F. *Am. Soc. Artif. Intern. Organs* **1980**, *3*, 160–175.
- (61) Baszkin, A.; Lyman, D. J. *J. Biomed. Mater. Res.* **1980**, *14* (4), 393–403.
- (62) Oreskes, I.; Singer, J. *Arthritis Rheum.* **1960**, *3* (3), 273–274.
- (63) Ariola, F. S.; Krishnan, A.; Vogler, E. A. *Biomaterials* **2006**, *27* (18), 3404–3412.
- (64) Brewer, S. H.; Glomm, W. R.; Johnson, M. C.; Knag, M. K.; Franzen, S. *Langmuir* **2005**, *21* (20), 9303–9307.
- (65) Kekicheff, P.; Ducker, W. A.; Ninham, B. W.; Pileni, M. P. *Langmuir* **1990**, *6* (11), 1704–1708.
- (66) Malmsten, M. M. *Colloids Surf., B* **1995**, *3*, 297–308.